 

*INTERACTION OF LASER RADIATION WITH MATTER. LASER PLASMA*

PACS numbers: 73.20.Mf; 42.25.Fx
DOI: 10.1070/QE2005v035n01ABEH002833

# Peculiarities of excitation of surface plasmons upon noncollinear light scattering

A.V. Andreev, A.A. Korneev, L.S. Mukina, M.M. Nazarov, I.R. Prudnikov, A.P. Shkurinov

*Abstract*. **The efficiency of excitation of surface plasmons upon noncollinear light scattering from a metal diffraction grating is studied. It is shown that this efficiency strongly depends on the grating profile and the azimuthal angle of rotation. The relation between the spatial configuration of the electromagnetic field near the grating – vacuum interface and the possibility of excitation of plasmons is found. Taking into account different conditions for plasmon excitation, the peculiarities of experimental angular dependences of specular reflection are explained.**

***Keywords***: *surface plasmons, diffraction grating, noncollinear light scattering*.

## 1. Introduction

Surface plasmons are surface electromagnetic waves (SEWs), which can be excited, under certain conditions, at the interface between two media [1, 2]. A SEW propagates along the interface and its amplitude exponentially decays upon moving away from the interface deep into both media. Excitation of the SEW is accompanied by a strong (by an order of magnitude) increase in the intensity of the electromagnetic field in a thin layer (a few tens of nanometres) near the interface and is manifested as a minimum in the angular or frequency dependence of specular reflection. For diffraction gratings, this phenomenon has been known as the Wood anomalies since 1902 [3]. From the moment of their first observation until present, SEWs are the object of numerous experimental and theoretical studies [4 – 6], which is connected with the prospects for the development of new methods for studying surfaces based on excitation of surface plasmons. These methods include, for example, the plasmon microscopy of surfaces [7] and plasmon fluorescence spectroscopy of thin films deposited on a metal diffraction grating [8]. There also exists the possibility of fabricating a waveguide based on a two-dimensional surface grating made of nanoparticles, in which surface plasmon waves can propagate [9].

**A.V. Andreev, A.A. Korneev, L.S. Mukina, M.M. Nazarov, I.R. Prudnikov, A.P. Shkurinov** Department of Physics, M.V. Lomonosov Moscow State University, Vorob'evy gory, 119992 Moscow, Russia;
e-mail: prudnik@phys.msu.ru

Received 12 July 2004; revision received 3 November 2004
*Kvantovaya Elektronika* **35** (1) 27 – 32 (2005)
Translated by M.N. Sapozhnikov

A local increase in the intensity of the electromagnetic field near the interface caused by a propagating SEW leads to the enhancement of a nonlinear-optical response of the surface [10], thereby increasing the efficiency of generation of optical harmonics, sum frequency, and multiwave mixing (see, for example, [4] and references therein). Therefore, the determination of optimal conditions for excitation of surface plasmons is undoubtedly also important for studying the nonlinear-optical response of the surface.

In this paper, we studied analytically the efficiency of excitation of plasmons in the case of noncollinear geometry, when grooves of a metal diffraction grating are parallel to the plane of incidence, the SEW is excited by an S-polarised light wave (the electric field vector is perpendicular to the plane of incidence). This study was stimulated by our recent experiments [4], in which we observed a strong enhancement of the nonlinear-optical response of a metal diffraction grating upon noncollinear excitation of SEWs.

This paper is a continuation of Ref. [4] and explains the asymmetric shape of the angular dependences of the SEW resonance at a small deviation from a symmetric noncollinear geometry of the experiment. Note that by now the excitation of plasmons only in a collinear scheme (grooves of the grating are perpendicular to the plane of incidence), when light is incident almost normally on a sample, is studied in detail both theoretically and experimentally. As an example, we mention Refs [11, 12] where it has been shown that the second spatial Fourier harmonic of the grating profile causes the diffraction interaction of plasmons and the appearance of the band gap – the frequency band where plasmons cannot be excited. In the case of a sinusoidal relief and normal incidence of light on a sample, only one minimum, related to the plasmon excitation, appears in the specular reflection spectrum upon variation of the light frequency. When the relief shape differs from sinusoidal, the plasmon resonance splits and two (dips) minima appear in the general case in the specular reflection spectrum [5, 11 – 14]. The distance between these two minima determines the width of the band gap.

In this paper, we studied the dependence of the plasmon excitation efficiency in a noncollinear scheme on the profile of a non-sinusoidal diffraction grating and the azimuthal angle of rotation around the normal to the grating surface, calculated the local intensity of the electromagnetic field near the diffraction grating – vacuum interface and found that the grating-relief profile and spatial distribution of the electromagnetic field substantially affect the efficiency of plasmon excitation. It is shown that our analytic approach correctly describes a number of specific features observed in

experiments on excitation of plasmons upon linear reflection of light.

## 2. Excitation of plasmons in a noncollinear scheme and formation of a band gap

Consider excitation of a SEW upon scattering of light from a metal diffraction grating in the noncollinear geometry. The geometry of light scattering is shown schematically in Fig. 1. In this scheme, the angle $\varphi$ between the reciprocal lattice vector $\boldsymbol{Q}$ and the normal $\boldsymbol{n}$ to the plane of light incidence can be varied within $-10^\circ \leqslant \varphi \leqslant 10^\circ$ around zero. The reciprocal lattice vector $\boldsymbol{Q}$ is directed perpendicular to the grooves of the diffraction grating. When $\varphi = 0$, and $\boldsymbol{Q} \| \boldsymbol{n}$ and the grating grooves are parallel to the plane of light incidence, there exists for a certain radiation frequency $\omega$ the angle of incidence $\vartheta$ at which noncollinear excitation of a SEW occurs in a strictly symmetrical scheme (Fig. 2).

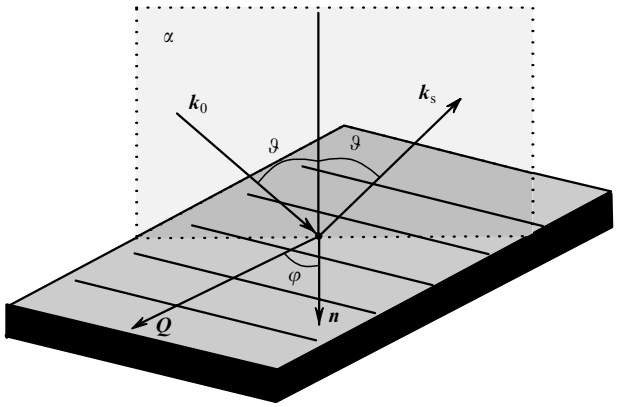


**Figure 1.** Scheme of scattering of light from a diffraction grating: $\alpha$ is the plane of incidence; $\boldsymbol{n}$ is the normal to the plane of incidence; $\boldsymbol{k}_{0,s}$ are the wave vectors of the incident and specular reflected waves; $\vartheta$ is the angle of incidence; $\boldsymbol{Q}$ is the reciprocal lattice vector perpendicular to the grooves of the diffraction grating; $\varphi$ is the azimuthal angle.

Let us analyse the mutual influence of plasmons in the case of noncollinear geometry of excitation of SEWs for $\varphi = 0$. We assume for certainty that the frequency $\omega$ of incident light is fixed and only the angle $\vartheta$ is changed. It is known [1, 2] that the modulus of the wave vector of a surface plasmon is described by the expression $K = (\omega/c)[\varepsilon_1\varepsilon_2/(\varepsilon_1 + \varepsilon_2)]^{1/2}$, where $\varepsilon_{1,2}$ are the dielectric constants of the metal and medium over the diffraction grating. To excite a SEW, the phase-matching condition

$$\boldsymbol{K}_{\pm 1} = \boldsymbol{k}_\tau \pm \boldsymbol{Q} \tag{1}$$

should be fulfilled [1, 2], where $\boldsymbol{k}_\tau$ is the tangential (to the diffraction grating plane) component of the wave vector $\boldsymbol{k}_0$ ($k_\tau = k_0 \sin\vartheta$, $k_0 = \omega/c$) of the incident wave; $Q = 2\pi/T$ is the modulus of the reciprocal lattice vector; and $T$ is the diffraction grating period. We changed the tangential component $\boldsymbol{k}_\tau$ of the wave vector of the incident wave to achieve phase matching, by varying the angle of incidence $\vartheta$ at the fixed frequency $\omega$. For $\varphi = 0$, two SEWs with the wave vectors $\boldsymbol{K}_{\pm 1}$, $K_{\pm 1} = K$ can be excited simultaneously (Fig. 2). The angle of incidence at which the SEW can be excited is determined from the condition $K = (k_\tau^2 + Q^2)^{1/2}$.

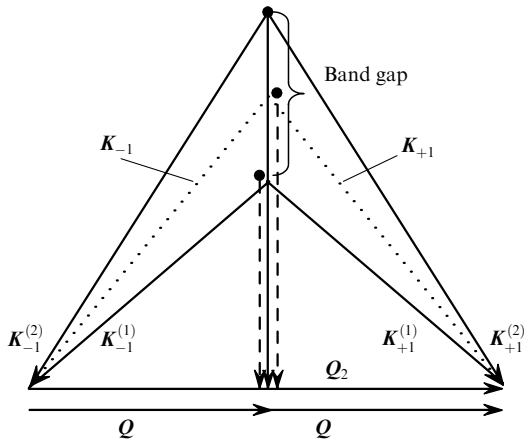


**Figure 2.** Scheme of the formation of the band gap: $\boldsymbol{Q}$ is the reciprocal lattice vector; $\boldsymbol{Q}_2 = 2\boldsymbol{Q}$ is the reciprocal grating vector for the second spatial Fourier harmonic of the relief; $\boldsymbol{K}_{\pm 1}$ are the wave vectors of SEWs in the zero approximation (degenerate case). Due to diffraction from a grating with the vector $\boldsymbol{Q}_2$ ($\boldsymbol{K}_{\pm 1} = \boldsymbol{K}_{\mp 1} \pm \boldsymbol{Q}_2$), SEWs with the wave vectors $\boldsymbol{K}_{\pm 1}^{(1)}$, $\boldsymbol{K}_{\pm 1}^{(2)}$ appear and the band gap is formed. The origin of the wave vector cannot lie on the segment indicated by the brace. The dashed straight lines show the tangential (in the diffraction grating plane) components of the wave vector of the incident wave.

If the surface relief differs from sinusoidal and is also characterised by the second spatial Fourier harmonic with the reciprocal grating vector $\boldsymbol{Q}_2 = 2\boldsymbol{Q}$, the SEW experiences efficient scattering with the diffraction vector $\boldsymbol{Q}_2$: $\boldsymbol{K}_{\pm 1} = \boldsymbol{K}_{\mp 1} \pm \boldsymbol{Q}_2$ (Fig. 2). Due to scattering of the SEW with the wave vector $\boldsymbol{K}_{-1}$, a SEW with the wave vector $\boldsymbol{K}_{-1} + \boldsymbol{Q}_2$ appears. Because phase matching $\boldsymbol{K}_{+1} = \boldsymbol{K}_{-1} + \boldsymbol{Q}_2$ takes place (Fig. 2), the latter SEW strongly affects the amplitude of the electromagnetic field of another SEW propagating with the wave vector $\boldsymbol{K}_{+1}$. The scattering of a SEW with the wave vector $\boldsymbol{K}_{+1}$ can be analysed similarly. Such an interrelation between the two SEWs removes degeneracy and results in the formation of a band gap (see also paper [11] where the appearance of the band gap in the collinear scheme of plasmon excitation was studied).

Note that the band gap is classically defined in the frequency domain [15]. However, for most of the periodic structures the concept of the band gap can be also introduced for the angular representation because the projection of the wave vector of the incident wave on the reciprocal lattice vector is determined both by the frequency and the angle of incidence. For this reason, a plane monochromatic wave in some range of the angles of incidence cannot reflect from the structure or propagate through it. In this paper, we define the band gap as a range of the angles of incidence of monochromatic radiation within which, despite the fulfilment of phase-matching condition (1), a SEW cannot be excited.

The removal of degeneracy means that instead of the two SEWs with the wave vectors $\boldsymbol{K}_{\pm 1}$, the four SEWs with the wave vectors $\boldsymbol{K}_{\pm 1}^{(1)}$ and $\boldsymbol{K}_{\pm 1}^{(2)}$, and $K_{+1}^{(1)} = K_{-1}^{(1)}$, $K_{+1}^{(2)} = K_{-1}^{(2)}$ appear in the general case (see Fig. 2). We will call SEWs with the waves vectors $\boldsymbol{K}_{\pm 1}^{(1)}$ and $\boldsymbol{K}_{\pm 1}^{(2)}$ SEW1 and SEW2, respectively. The band gap (in the angle of incidence) is conventionally shown in the wave-vector space in Fig. 2. The wave vector of a SEW cannot originate inside this zone. Let $\vartheta_1$ and $\vartheta_2$ be the angles of incidence at which the SEW1

and SEW2 are excited. It follows from Fig. 2 that $\vartheta_1 < \vartheta_2$ and the difference $\vartheta_2 - \vartheta_1$ determines the width of the band gap in angular units. Note that band gaps formed upon scattering of SEWs in the cases of dynamic diffraction of X-rays in perfect crystals [16] and diffraction of light in photonic structures [15] appear due to similar processes.

The above qualitative conclusions are substantiated in the next sections of the paper by numerical simulations. It is shown that, depending on the surface relief and the angle $\varphi$, the generation efficiency of SEW1 and SEW2 can be substantially different, including the impossibility to excite a certain SEW in principle.

## 3. Method of calculations and the recurrence relation

The problem of noncollinear scattering of a plane electromagnetic wave from a periodic surface relief is essentially a vector problem. We used in calculations the method of solution of Maxwell's vector equations [4] based on the subdivision of the surface relief into $N$ thin layers of the same thickness $d$, the relief height being $H = Nd$. The layer thickness $d$ is selected so that the field weakly changes over the layer depth and reflection of light from the layer can be neglected. The reflection and transmission coefficients of individual inhomogeneous layers are calculated analytically using Maxwell's equations. The amplitude of the electric field reflected from a diffraction grating is calculated from the recurrence relation

$$\hat{R}_j = \hat{s}_j + \hat{\bar{\tau}}_j \hat{R}_{j+1} (\hat{1} - \hat{\bar{s}}_j \hat{R}_{j+1})^{-1} \hat{\tau}_j, \qquad (2)$$

where $\hat{s}_j$, $\hat{\tau}_j$ are the reflection and transmission coefficients of the $j$th layer, which are matrices. The bars over the coefficients indicate that they correspond to the wave incident on the back side of the layer. First the reflection coefficient $\hat{R}_N$ for a homogeneous layer (substrate) of a semi-infinite thickness is determined with the help of Fresnel formulae. The reflection coefficient $\hat{R}_0$ for the diffraction grating as a whole can be calculated by applying successively recurrence relation (2).

The above algorithm allows us to calculate the intensity of specular reflection of an electromagnetic wave of arbitrary polarisation as a function of the angle of incidence of the wave and the azimuthal angle of rotation of the diffraction grating around the normal. In addition, this approach permits the calculation of the local intensity distribution of the electromagnetic field near the spatially inhomogeneous interface between two media and the intensity of the nonlinear response of a spatially inhomogeneous medium.

## 4. Effect of the diffraction grating profile on the plasmon excitation efficiency

Consider the effect of the diffraction grating relief on excitation of a SEW under the condition $\varphi = 0$. We assume that the grating profile is described by the function

$$\xi(x) = 0.5H_1[1 + \cos(Qx)] + 0.5H_2[1 + \cos(Q_2 x + \psi)]. \qquad (3)$$

The phase $\psi$ changes within $0 \leqslant \psi \leqslant \pi$. If $\psi = 0$, $\pi$, then $\xi(x) = \xi(-x)$ and the relief has a symmetric shape. For other values of $\psi$, the grating profile is asymmetric. Figure 3 shows the dependences of specular reflection on the angle of incidence $\vartheta$ calculated for different values of the phase $\psi$. We used in calculations the following parameters of the grating and incident radiation: the wavelength of the S-polarised light was 780 nm, the diffraction grating made of gold had the period $T = 1.12$ μm, $H_1 = 90$ nm, and $H_2 = 0.2H_1$. One can see from Fig. 3 that in the case of a symmetric relief ($\psi = 0, \pi$), the specular reflection curve has only one minimum. This minimum is shifted to greater ($\psi = \pi$) or smaller ($\psi = 0$) angles of incidence $\vartheta$ compared to the case of a sinusoidal profile. Therefore, for $\psi = 0$, only SEW1 can be excited, whereas for $\psi = \pi$, only SEW2. If the relief symmetry is distorted, the specular reflection curve has two minima, indicating excitation of SEW1 and SEW2. One can see from Fig. 3 that the efficiency of plasmon excitation (the depth of minima) can be substantially different. The distance between the minima, i.e., the width of the band gap is determined by the second-harmonic amplitude $H_2$ in expression (3).

The peculiarities of the specular reflection curves can be explained by analysing the local intensity of the electric field $\boldsymbol{E}(\boldsymbol{r})\boldsymbol{E}^*(\boldsymbol{r})$ near the metal–vacuum interface. Figure 4 presents the two-dimensional maps of the distribution of the local intensity of the field in the vicinity of one groove of the grating, calculated for different grating profiles (different values of the phase $\psi$ between the first and second harmonics) and for the angles of incidence $\vartheta_1$ and $\vartheta_2$

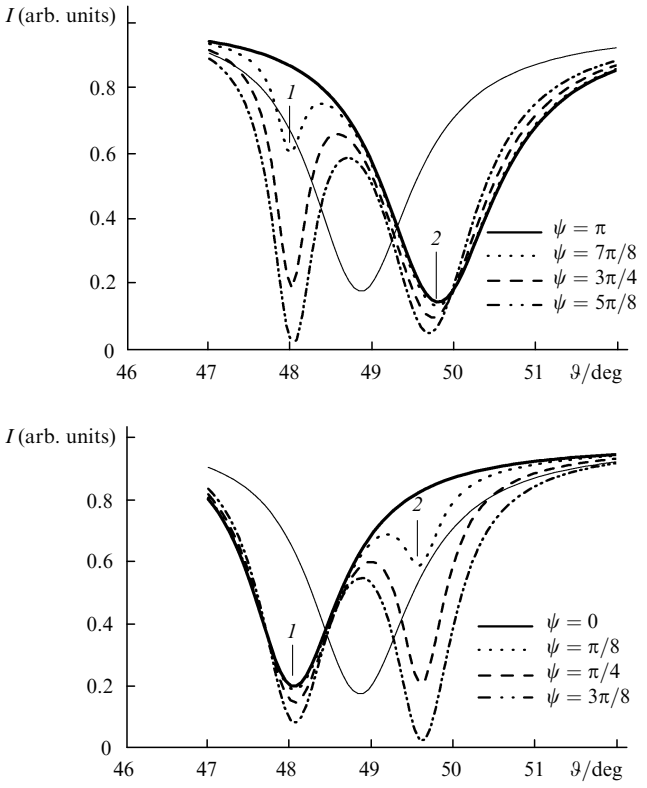


**Figure 3.** Dependences of the intensity of specula reflection of light on the angle of incidence $\vartheta$ calculated for $\varphi = 0$ (Fig. 1) and different profiles of a diffraction grating [see (3)]. The thin solid curve shows specular reflection in the case of a sinusoidal relief ($H_2 = 0$); (*1*) and (*2*) are the minima demonstrating excitation of SEWs with the wave vectors $\boldsymbol{K}_{\pm 1}^{(1)}$ and $\boldsymbol{K}_{\pm 1}^{(2)}$, respectively (Fig. 2); the parameters of the grating and incident radiation are presented in the text.

corresponding to the minima denoted by numbers (*1*) and (*2*) in Fig. 3. The plane of Fig. 4 corresponds to the *xz* plane. In this case, $\boldsymbol{x}||\boldsymbol{Q}$, and $\boldsymbol{z}$ is the normal to the grating surface. In the upper pictures in Fig. 4 ($\vartheta = \vartheta_1$), the main contribution to the field is made by SEW1, while in the middle pictures ($\vartheta = \vartheta_2$) the main contribution is made by SEW2. The lower pictures show the profiles of the second spatial harmonic taking into account its phase $\psi$. The light regions correspond to metal grooves of the grating, where the electromagnetic field does not penetrate.

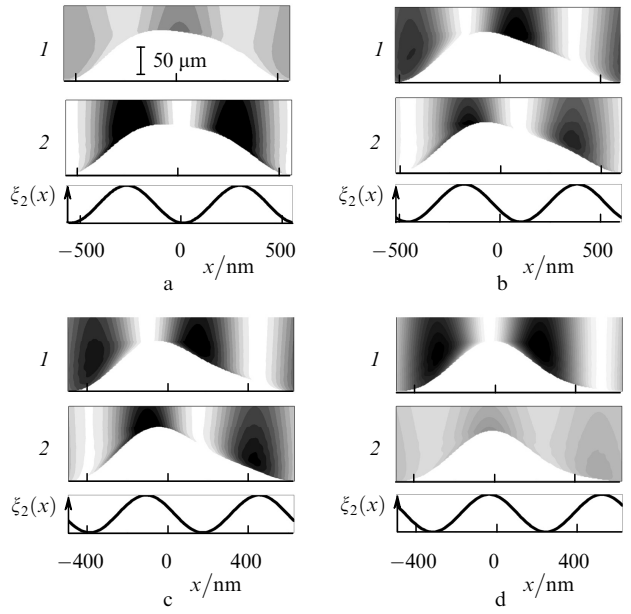


**Figure 4.** Distributions of the local intensity of the electric field in the region of a groove of the grating (section of the grating surface across grooves) calculated for different profiles of the diffraction grating [see (3)] and two angles of incidence corresponding to minima (*1*) (upper figures) and (*2*) (middle figures) (Fig. 3). The maximum intensity of the electromagnetic field of the SEW is indicated by dark colour. The lower figures show the second spatial harmonic of the profile $\xi_2(x) = \cos(Q_2 x + \psi)$ [see (3)]; the phase of the second spatial harmonic is $\psi = 7\pi/8$ (a), $5\pi/8$ (b), $3\pi/8$ (c), and $\pi/8$ (d).

One can see from Fig. 4 that a standing wave field is produced in the vicinity of the metal – vacuum interface. The position of antinodes of the standing field (*1*) always coincides with the minima of the second spatial harmonic of the relief. And vice versa, the antinodes of the standing field (*2*) are always 'located' at the peaks of the second harmonic of the relief. Therefore, the maxima of the intensity of fields (*1*) and (*2*) are displaced by the distance $T/4$ with respect to each other (Fig. 4). We determined the position of the field antinodes using the known numerical algorithms [17] for searching for the function extremum, the error of calculations being less than 1%. For a symmetric relief, when $\psi = 0$, the antinodes of the wave field (*1*) are located at the slopes of the diffraction grating. If the phase $\psi$ tends to zero, the maxima of the wave field (*2*) tend to occupy the position at the tops and troughs of the grating relief (Figs 4c, d). It can be shown that for $\psi = 0$, such a spatial configuration of the field (*2*) cannot be realised because it corresponds (in the limit $\psi \to 0$) to the distribution of the electric-field phase which is asymmetric with respect to the plane $x = 0$. In other words, when $\psi = 0$, SEWs1 cannot be excited because the problem is characterised by symmetry with respect to the plane $x = 0$. Similarly, in another 'limiting' case, for $\psi = \pi$, SEWs1 cannot be excited. If the relief symmetry is violated, both SEW1 and SEW2 can be excited (Fig. 4). Note that the above-described spatial modes of fields (*1*) and (*2*), which are locked to the phase of the second Fourier harmonic of the grating profile, appear in the case of collinear scattering of light as well [11, 12]. It is also interesting to point out similarity with the dynamic diffraction of X-rays in crystals, when the antinodes of a standing electromagnetic wave can be located on the atomic planes and between them [16].

## 5. Excitation of plasmons at different azimuthal angles

Let us analyse the plasmon excitation efficiency at different angles of rotation $\varphi$. For definiteness, we consider in detail the case of a symmetric relief [$\psi = 0$, see (3)]. Figure 5 shows the specular reflection curves calculated for different angles $\varphi$. One can see that the SEW2 generation efficiency increases with increasing $\varphi$. This is explained by the fact that a change in the azimuthal angle violates the 'symmetry' of the field incident on the grating and removes the prohibition on excitation of SEW2. Therefore, any violation of the symmetry of the scattering geometry allows excitation of two SEWs. The calculations of the electric-field intensity, similar to those presented in Fig. 4, show that for small angles ($\varphi \leqslant 0.1^\circ$), when the depth of minimum (*2*) is small, the antinodes of the wave field (*2*) are located near the profile slopes. As the angle $\varphi$ and the depth of minimum (*2*) increase (Fig. 5), the antinodes begin to shift and for $0.5^\circ \leqslant \varphi \leqslant 1^\circ$ they are located almost in troughs and peaks of the diffraction grating relief. For the values $\varphi \leqslant 1^\circ$ considered here, the antinodes of the wave field (*1*) are located on the slopes of the grating relief.

Figure 6 shows the intensities of specular reflection calculated as functions of the angles $\varphi$, and $\vartheta$. Figure 6b presents the intensity of light reflected from the sinusoidal relief: $H_2 \equiv 0$ – the case of degeneracy [see (3)]. Figure 6a clearly illustrates the region of angles $\vartheta$ corresponding to the band gap (see Fig. 2). In the presence of degeneracy, the

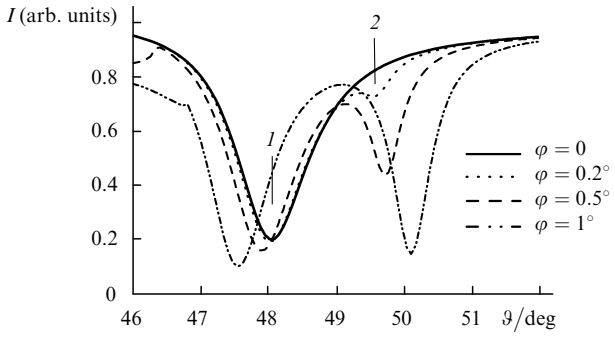


**Figure 5.** Dependences of the intensity of specular reflection of light from the diffraction grating with a symmetric profile [$\psi = 0$ in (3)] on the angle of incidence $\vartheta$ calculated for different azimuthal angles $\varphi$; (*1*) and (*2*) are the minima demonstrating excitation of SEWs with the wave vectors $\boldsymbol{K}_{\pm 1}^{(1)}$ and $\boldsymbol{K}_{\pm 1}^{(2)}$, respectively (Fig. 2). The parameters of the diffraction grating and incident radiation are presented in the text.

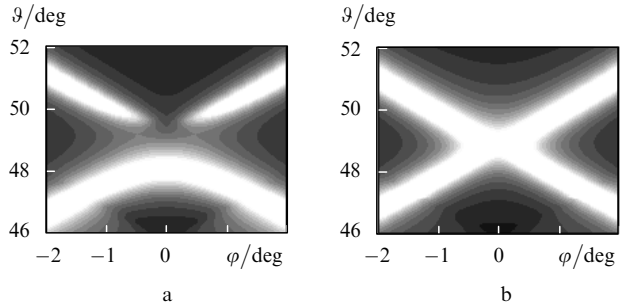


**Figure 6.** Dependences of the intensity of specular reflection of light from the diffraction grating on angles $\varphi$ and $\vartheta$ calculated for reflection from the grating with a symmetric profile [$\psi = 0$ in (3)] (a) and a sinusoidal profile, $H_2 \equiv 0$ [see (3)] (b). The maximum intensity is indicated by black colour. The parameters of the diffraction grating and incident radiation are presented in the text.

positions of minima in Fig. 6b are determined by the phase-matching condition (1).

It can be shown that in another 'limiting' case of a symmetric relief, when $\psi = \pi$, for $\varphi \neq 0$ the specular reflection curve has minimum (*1*), whose depth increases with increasing $\varphi$. In this case, the angular distance between minima (*1*) and (*2*) also increases.

## 6. Experimental examples

Figures 7 and 8 present the experimental data illustrating qualitatively the results obtained above. Note that the inverse problem of scattering from a diffraction grating, which allows one to obtain quantitative agreement between the theory and experiment, was not considered in this paper. The experimental sample was a gold film of thickness 30 nm deposited on a quartz diffraction grating. Experiments were performed using radiation at a wavelength of 780 nm. The parameters of the sample and experimental setup are described in detail in [4] (sample T6).

The experimental specular reflection curve (Fig. 7) corresponding to the angle $\varphi = 0$ has only minimum (*1*), in accordance with the calculated curve shown in Fig. 5. For $\varphi \neq 0$, minimum (*2*) appears, and for small angles ($\varphi \leqslant 1^\circ$) the depths of minima (*1*) and (*2*) are substantially different (Fig. 7). This asymmetry is caused by substantially different

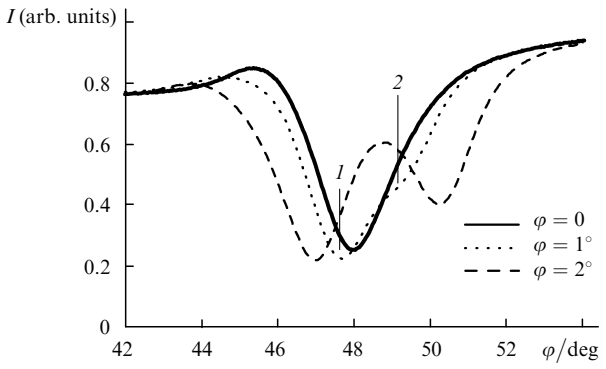


**Figure 7.** Experimental dependences of the specular reflection intensity on the angle $\vartheta$ obtained at different azimuthal angles $\varphi$. The parameters of the diffraction grating and experimental conditions are described in [4].

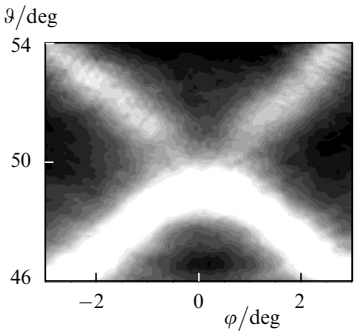


**Figure 8.** Experimental specular reflection of light from the diffraction grating [4] as a function of angles $\varphi$ and $\vartheta$. The maximum intensity of the reflected wave is indicated by black colour.

excitation conditions for SEW1 and SEW2 (see section 5 and Fig. 5). The interaction of SEWs causes the splitting of the plasmon resonance and the appearance of the band gap – the region of angles $\vartheta$ where SEWs cannot be excited. The band gap is clearly seen in the experiment (Fig. 8) and is confirmed by calculations (Fig. 6a).

## 7. Conclusions

We have shown that surface plasmons, or SEWs, excited upon noncollinear scattering of light from a metal diffraction grating, experience scattering involving the second spatial harmonic of the grating relief. The interaction of SEWs causes the splitting of the degenerate plasmon resonance and the formation of the band gap – the region of angles of incidence where SEWs cannot be excited. The splitting of the plasmon resonance results in the appearance of two modes of a standing wave field near the metal – vacuum interface. The antinodes of one of the modes coincide with the maxima and of another mode with the minima of the second spatial harmonic of the grating relief. By varying the angle of incidence of light on the grating and (or) the angle of rotation of the grating, one can successively excite these modes and control the field distribution in the vicinity of the grating – vacuum interface. The peculiarities of the spatial distribution of the field modes determine the SEW excitation efficiency, whose excitation can be even prohibited. These peculiarities can be used to increase the nonlinear-optical response, in the spectroscopy of inhomogeneous films, and for diagnostics of a periodic metal surface.

## References

1. Raether H. *Surface Plasmons on Smooth and Rough Surfaces and on Gratings* (Berlin: Springer-Verlag, 1988) Vol. 111.
2. Shalaev V.M. *Nonlinear Optics of Random Media: Fractal Composites and Metal-Dielectric Films* (Springer Tracts in Modern Physics, Berlin: Springer, 2000) Vol. 158.
3. Wood R.W. *Philos. Mag.*, **4**, 396 (1902).
4. Andreev A.V., Nazarov M.M., Prudnikov I.R., Shkurinov A.P., Masselin P. *Phys. Rev. B*, **69**, 035403 (2004).
5. Sychugov V.A., Tishchenko A.V., Usievich B.A., Salakhutdinov I.F. *Pis'ma Zh. Eksp. Teor. Fiz.*, **62**, 794 (1995).
6. Seminogov V.N., Sokolov V.I. *Opt. Spektr.*, **68**, 88 (1990).
7. Somekh M.G., Liu S.G., Velinov T.S., See C.W. *Opt. Lett.*, **25**, 823 (2000).
8. Kreiter M., Neumann T., Mittler S., Knoll W., Sambles J.R. *Phys. Rev. B*, **64**, 075406 (2001).

9. Bozhevolnyi S.I., Erland J., Leosson K., Skovgaard P.M.W., Hvam J.M. *Phys. Rev. Lett.*, **86** 3008 (2001).
10. Shen Y.R. *The Principles of Nonlinear Optics* (New York: Wiley, 1984).
11. Barnes W.L., Preist T.W., Kitson S.C., Sambles J.R. *Phys. Rev. B*, **54**, 6227 (1996).
12. Kreiter M., Mittler S., Knoll W., Sambles J.R. *Phys. Rev. B*, **65**, 125415 (2002).
13. Zhizhin G.N., Sychugov V.A., Silin V.I., Yakovlev V.A. *Kvantovaya Elektron.*, **11**, 1411 (1984) [*Sov. J. Quantum Electron.*, **14**, 952 (1984)].
14. Sychugov V.A., Klimov M.S., Svakhin A.S. *Trudy IOFAN*, **34**, 147 (1991).
15. Yablonovitch E. *Phys. Rev. Lett.*, **58**, 2059 (1987).
16. Pinsker Z.G. *Rentgenovskaya kristallooptika* (X-Ray Crystal Optics) (Moscow: Nauka, 1982).
17. Press W.H., Teukolsky S.A., Vetterling W.T., Flannery B.P. *Numerical Recipes in Fortran 77: The Art of Scientific Computing* (Cambridge: Cambridge University Press, 1992).